# The Theory of Atomic and Molecular Collisions

**John N. Murrell**
*School of Chemistry and Molecular Sciences, University of Sussex, Falmer, Brighton BN1 9QJ*
**S. Danko Bosanac**
*Ruder Boskovic Institute, P.O. Box 1016, 41001 Zagreb, Croatia*

## 1 Interatomic and Intermolecular Potentials

The interaction of atoms, either individually or as components of molecules, is determined by potentials which are functions of the relative positions of these atoms. The cohesion of liquids and solids, the sticking of molecules to surfaces, the transport of heat in gases, chemical reactivity; all of these can in principle be explained or predicted if these potentials are known. For some of these phenomena we only need to determine the dynamics of bimolecular collisions; others, such as the melting of a solid, are macroscopic properties and one needs to involve the statistical behaviour of $\sim 10^{23}$ atoms or molecules.

All observable properties such as those mentioned above can be used on a trial and error basis to determine features of the potential: take a potential, calculate the property, and compare with experimental observations. If the agreement is good then a certain range of the potential will be satisfactory. However, individual properties are not sufficiently sensitive to all features of the potential, so in general one will need to measure a potential against several different properties before one can be satisfied with it. The connection between atomic and molecular properties and interatomic or intermolecular potentials is a subject generally referred to as the theory of intermolecular forces, and this has been frequently reviewed.[1] In this review we examine an important part of this subject, namely the dynamics of atomic and molecular bimolecular collisions in crossed-beam experiments. The reason for its importance is that this type of experiment can in principle provide a more sensitive test of potentials than any other.

If one takes two beams of molecules with narrow ranges of velocities, and with the molecules all in the same quantum state (electronic, vibrational, and rotational state as appropriate), and after crossing these beams in a vacuum chamber measures the distribution of products as a function of angle relative to the incident beams, each product being separately identified not only for its molecular composition but also for its individual quantum state, then that is a great deal of information. If the experiment is performed for several collision velocities and for several initial quantum states then we have even more data, and all of this can in principle be explained by potential functions, perhaps even a single potential function.

Let us first be a little more formal about the term potential. An important element of theories of molecular spectroscopy and reactivity is the Born–Oppenheimer approximation that the motion of electrons and nuclei can be treated as separate but linked problems. The basis for this is that nuclei have a much larger mass than the electron so that their motion is sluggish compared with the motion of electrons. We can conclude that electronic states (their wave functions and energies) adjust smoothly and instantaneously to movements of the nuclei. These energies, when added to the repulsion of the nuclei, provide a potential which governs the nuclear motion.

There are certain features of spectroscopy that can only be explained by going beyond the Born–Oppenheimer approximation. In these cases the quantum states cannot be identified with a unique electronic wave function. Likewise, there are chemical reactions in which the electronic state changes somewhere in the passage from reactants to products; these reactions are usually referred to as non-adiabatic but they will not be covered in this review.

*Professor Murrell (B.Sc., Ph.D., F.R.S.C.) is a theoretical chemist whose research interests have covered many branches of valence theory, spectroscopy, and the states of matter. He has written seven books on these topics, the most recent of which are on potential energy functions and scattering theory; these are now the main topics of his research. He was elected a Fellow of the Royal Society in 1991.*

*Professor Bosanac obtained his first degree in theoretical physics from the University of Zagreb in 1968 and his Ph.D. from Sussex University in 1972. He was Lady Davis Fellow at the Hebrew University of Jerusalem in 1977/78. His present research interests include the dynamics of molecular collisions, interaction of radiation with matter, and the general aspects of the classical and quantum theories.*

## 2 The Theoretical Tools

Three theoretical techniques are available for calculating the motion of nuclei on a potential energy surface; classical mechanics, quantum mechanics, and semi-classical mechanics. Our picture in classical mechanics is that of the snooker table; but the atoms are not hard spheres and the motion is in three dimensions not two. Our picture of collisions in quantum mechanics is of waves breaking around a lighthouse, and we interpret the calculations using the fundamental postulate of quantum mechanics that the probability of events is obtained by squaring the wave functions.

Quantum mechanics has a well defined classical limit when the de Broglie wavelength of the particle, $\lambda = h/p$, is small compared with the range of the potential. For example, a hydrogen atom, moving with a kinetic energy of 0.1 eV has a wavelength of approximately 1 Å which is comparable to interatomic distances. One would therefore expect to see wavelike properties from the collision of such atoms with molecules or solids; such properties as diffraction and interference. Heavier atoms and higher energies will make these properties more difficult to see and in such cases the classical picture is appropriate. Quantum mechanics always operates, even for heavy particles. The question is whether the characteristic quantum phenomenon can be resolved in the experiment.

The simplest formulation of classical mechanics when the interaction potential is complicated and the equations have to be solved numerically is that provided by Hamilton's equations. These govern the time dependence of the coordinates $q$ and momenta $p$ of the particles; a set of variables $q(t)$, $p(t)$. For $N$ atoms at a given time these variables are represented by a point in $6N$ dimensional space, and this point moves along a path which is called a trajectory that can be calculated by solving Hamilton's equations.

Hamilton's equations are coupled first-order differential equations of the form

$$\frac{\mathrm{d}q_i}{\mathrm{d}t} = \frac{\partial H}{\partial p_i} \qquad (1)$$

$$\frac{dp_i}{dt} = -\frac{\partial H}{\partial q_i} \quad (2)$$

where $H$ is the Hamiltonian, which is the sum of the algebraic expressions for the kinetic and potential energies

$$H = T + V \quad (3)$$

If $V$ is very simple, say a constant or a harmonic function, equations (1) and (2) can be solved analytically. In other cases they must be solved numerically by taking a step by step evolution of the trajectory $[q(t),p(t)]$ using a Taylor expansion of the variables.

There are two Schrödinger equations in quantum mechanics. The one most familiar to chemists is the time-independent equation which governs the so-called stationary states or eigenstates of the system. This is commonly written

$$\boldsymbol{H}\psi(q) = E\psi(q) \quad (4)$$

where $\boldsymbol{H}$ is the quantum mechanical Hamiltonian and $\psi$ is the wavefunction.

Schrödinger's second equation, called the time-dependent equation, describes the time evolution of the wave function in a non-stationary state of the system and is

$$-\frac{\hbar}{i}\frac{\partial\psi(q,t)}{\partial t} = \boldsymbol{H}\psi(q,t) \quad (5)$$

At first sight it may appear that the time-dependent Schrödinger equation is more appropriate to the scattering experiment than the time-independent equation; molecules come from a source, collide with one another, and are scattered into a detector. If the experiment is to fire pulses of molecules into the scattering chamber and to measure not only the angular distribution of the products but also their time of arrival at the detector, then the time-dependent equation is needed. However, an alternative scattering experiment is to have a continuous stream of molecules coming from the source, and after scattering, arriving at the detector. This experiment has no time evolution; a snapshot at any time shows the same situation. In this case the observable properties can be obtained by solving the time-independent Schrödinger equation; both give the same scattering angles. Currently the time-independent approach is more favoured because normally it is computationally the simpler approach. Moreover, all the concepts of scattering theory except collision time emerge from this approach and for these reasons we only use the time-independent approach in this review.

Scattering is always a multidimensional problem; even for atomic collisions one has both radial (distance between the atoms) and angular variables, and for molecular collisions one also has variables to describe vibrational and rotational states. The computational demands in scattering increase rapidly with the number of variables, so that atom–molecule scattering is much more difficult than atom–atom, and if atoms are exchanged in the scattering process, there is another increase in difficulty.

Quantum mechanical probabilities show the characteristics of interference; these are oscillations in the probability which arise from cross terms when one squares a wave function. In classical mechanics one calculates probabilities directly from trajectories. To get interference from classical mechanics one would have to take the square root of the probability, but without further information this is undefined to within a phase factor $\phi$, for we note

$$|P^{\frac{1}{2}}e^{i\phi}|^2 = P \quad (6)$$

Semi-classical mechanics provides a recipe for assigning a phase $\phi$ to a classical trajectory. The origins of this lie in the old quantum theory of atoms developed by Bohr. His recipe for quantization can be written

$$\oint p\,dq = nh \quad (7)$$

where $n$ is an integer and the integral, called the action integral, is taken over a complete orbit. In semi-classical mechanics we calculate the phase associated with a classical trajectory by the formula

$$\phi = \hbar^{-1}\int_{q_i}^{q_f} p\,dq \quad (8)$$

This result can be proved by taking the classical limit of quantum mechanics ($h \to 0$) and deriving what is called the JWKB approximation to the wave function.

## 3 Types of Collision

The simplest type of scattering experiment to treat theoretically is the collision of two atoms when there is no transfer of charge and no change in the electronic states of the atoms. We call these collisions elastic, the term implying that there is no change in the internal energies of the colliding species.

In a collision, atoms will change their individual translational energies; but if the positions of the two atoms are $\boldsymbol{r}_1$ and $\boldsymbol{r}_2$ (vectors referred to space fixed coordinates) then the positions of the centre of mass is

$$\boldsymbol{R} = (m_1\boldsymbol{r}_1 + m_2\boldsymbol{r}_2)/(m_1 + m_2) \quad (9)$$

and the vector of their relative separation is

$$\boldsymbol{r} = \boldsymbol{r}_1 - \boldsymbol{r}_2 \quad (10)$$

Using these variables, called a centre-of-mass or molecule-fixed system the translational energies associated with $\boldsymbol{R}$ and $\boldsymbol{r}$ are separately conserved.

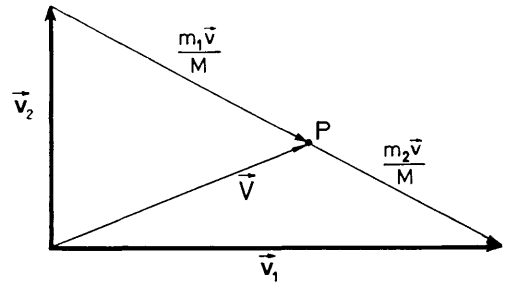


**Figure 1** Newton diagram for the transformation from laboratory ($v_1$,$v_2$) to centre-of-mass velocities ($V$,$v$). The laboratory beams have been taken as perpendicular.

Figure 1 shows the relationship between the velocity vectors; so-called Newton diagram. In the laboratory we measure the deflection angle $\theta_L$ of one of the beams (1, say). What we calculate from theory is the deflection angle $\theta_C$ of the relative velocity vector; $v$ does not change its length on collision as do $v_1$ and $v_2$. The relationship between the two is shown in Figure 2. To compare theory with experiment we always have to make this transformation from centre-of-mass to laboratory systems; it is a little more complicated if there is a change in internal energy on collision (for then the length of $v$ changes) or if there is a change of mass (for then the ratio of the two components of $v$ about the centre of mass point P will change).

In an inelastic collision there is an exchange of energy between the translational motion of the colliding species and their internal states but no exchange of atoms. Rotational energy spacings are typically $10^{-2}$ eV, and vibrational energy spacings typically $10^{-1}$ eV. If there is sufficient energy in the collision to excite vibrations, then rotational energies will also change.

In reactive scattering there is the added complication that the

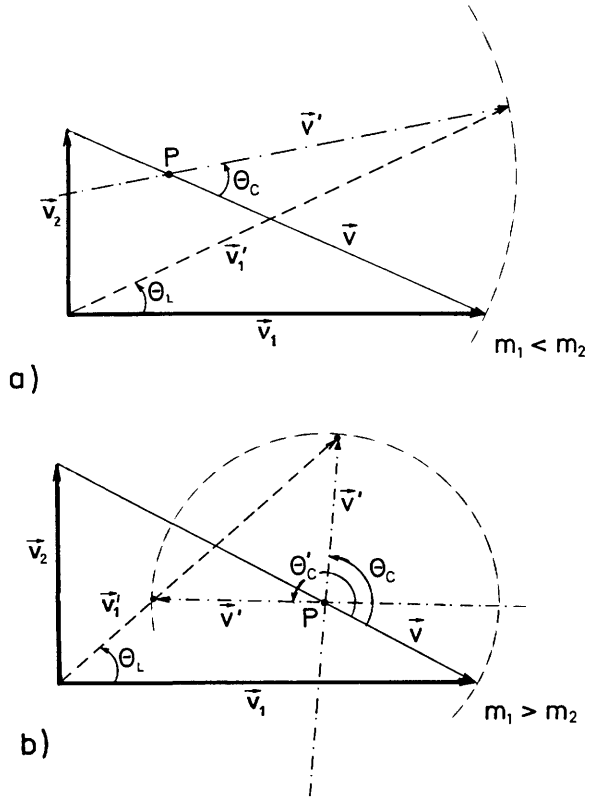


**Figure 2** Transformation from laboratory to centre-of-mass velocities for elastic scattering. When $m_1 < m_2$ there is a unique $\theta_C$ for each $\theta_L$; if $m_1 > m_2$ there are two possible values of $\theta_C$ for each $\theta_L$.

coordinates describing rotations and vibrations will be different for reactants and products, and that complicates considerably the solution of the quantum mechanical problem.

To summarize: we have three types of collision which in order of complexity are elastic, inelastic and reactive; we have three types of theory which in order of computational difficulty are classical, semi-classical, and quantum. For elastic scattering of atoms we can easily carry out all three types of calculation and make useful comparisons of the results. At the other extreme, for reactive scattering only classical calculations are easy, and it is only in recent years that full quantum mechanical calculations have become feasible.

The formal proofs of mathematical relationships and descriptions of the numerical methods used to calculate scattering cross sections are not given in this review. Most are covered in our own book on the subject[2] and there are many other valuable texts, mostly written at the postgraduate level.

## 4 Atom–Atom Elastic Scattering; Classical Mechanics

Figure 3 shows a typical classical trajectory (cm coordinates) for two atoms interacting under a repulsive potential. A particle of

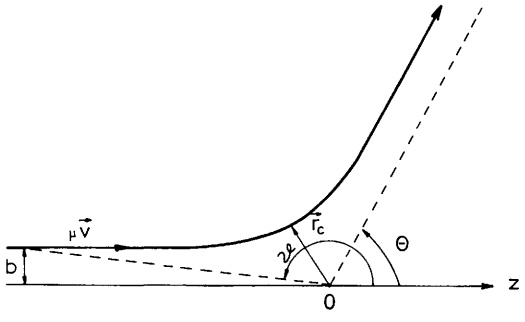


**Figure 3** Parameters for central field scattering.

effective mass $\mu = m_A m_B/(m_A + m_B)$ comes in along a line parallel to the $z$-axis in the $xz$ plane, is scattered by $V(r)$ centred at O, and disappears to infinity along a line making an angle $\theta$ with the $z$-axis; $\theta$ is called the deflection angle.

The kinetic energy of relative motion is

$$T = \tfrac{1}{2}\mu v^2 = \tfrac{1}{2}\mu \dot{r}^2 = \frac{1}{2}\mu(\dot{x}^2 + \dot{z}^2) \tag{11}$$

where $\dot{r} = dr/dt$, *etc.* It is easier to solve the problem in polar than in cartesian coordinates, so writing

$$x = r\sin\theta,\ z = r\cos\theta \tag{12}$$

and taking derivatives with respect to time we find

$$T = \tfrac{1}{2}\mu(\dot{r}^2 + r^2\dot{\theta}^2) \tag{13}$$

The total energy is obtained by adding to this the potential,

$$E = \tfrac{1}{2}\mu(\dot{r}^2 + r^2\dot{\theta}^2) + V(r) \tag{14}$$

The angular momentum of the system is defined by the vector product

$$\boldsymbol{L} = \mu \boldsymbol{r} \times \boldsymbol{v} \tag{15}$$

which is directed along the $y$ axis. Angular momentum like the energy is unchanged during the trajectory. In polar coordinates its magnitude is

$$L = \mu r^2\dot{\theta} \tag{16}$$

and if this is introduced into equation 14 we have

$$E = \frac{1}{2}\mu\dot{r}^2 + \frac{L^2}{2\mu r^2} + V(r) \tag{17}$$

$L^2/2\mu r^2$ is the centrifugal potential; it acts as a repulsive component, which has to be added to the central force potential when we solve the dynamics as a one-dimensional problem in $r$.

Figure 4 shows some effective potentials $V_L(r)$ for several values of $L$. $V(r)$ generally decays faster than the centrifugal potential at large $r$; typically as $r^{-6}$ so that for non-zero $L$ the centrifugal potential is always the dominant term at large $r$, the exception being potentials between ions. For small values of $L$ there is a centrifugal barrier at large $r$ and the centrifugal potential reduces the depth of the potential well (as in Figures 4b and 4c). At some critical value of $L$ the centrifugal potential is just large enough to remove completely the well in the effective potential (as in Figure 4d) so for values of $L$ above this, $V_L(r)$ is wholly repulsive.

The dashed line in Figure 4 shows a possible collision energy and we can think of the atoms coming in along this line from $r = \infty$ until they meet $V_L(r)$. This point, the smallest value of $r$ in the trajectory, is called the classical turning point ($r_c$ in Figure 3), for after this $r$ increases with time as the atoms depart from each other to infinity. At small values of $L$, $r_c$ occurs in the repulsive region of the potential well, but for large $L$ the classical turning point occurs in the region of the centrifugal barrier. Whether or not a trajectory surmounts a centrifugal barrier or not depends on the collision energy. However, at large $L$ the classical turning point is always determined by the centrifugal barrier.

From equation 16 we obtain an expression for $\dot{\theta}$ and from equation 17 an expression for $\dot{r}$ and dividing one by the other we obtain

$$\frac{d\theta}{dr} = \frac{\dot{\theta}}{\dot{r}} = \pm\frac{L}{\mu r^2\{2(E - V_L(r)\}^{\frac{1}{2}}} \tag{18}$$

The positive sign applies to the inward part of the trajectory ($r$ decreases as $\theta$ decreases) and the negative sign to the outward

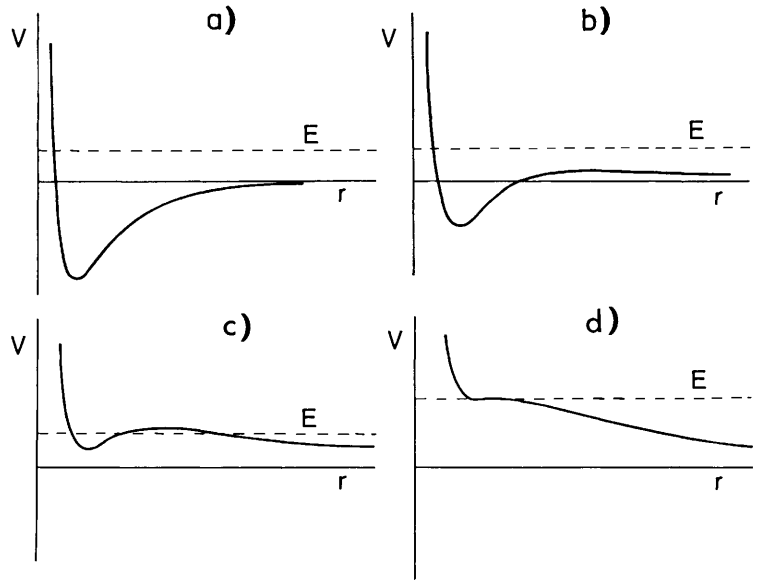


**Figure 4** Effective potentials for atom–atom scattering. (a) $L = 0$; (b), (c), (d) $L \neq 0$. (a) and (b) have one classical turning point, (c) has three turning points, and (d) shows an inflection point ($L = 55$).

part. If we integrate from $r = \infty$ ($\theta = \pi$) to the classical turning point ($r = r_c$) and then back to infinity the final value of $\theta$ will be the deflection angle. Writing the total integral over $r$ as twice the integral from $r_c$ to $\infty$, we have

$$\theta(E,L) = \pi - 2\int_{r_c}^{\infty} \frac{L\mathrm{d}r}{\mu r^2\{2[E - V_L(r)]\}^{\frac{1}{2}}} \tag{19}$$

It is useful to introduce an important quantity, labelled $b$ in Figure 3, called the impact parameter. A head-on collision has $b = 0$, a complete miss is at such a large value of $b$ that $V(b) = 0$. The angular momentum, energy, and impact parameter are related by

$$L = b\mu v = b(2\mu E)^{\frac{1}{2}} \tag{20}$$

so that the expression for the deflection angle can be written in terms of $E$ and $b$ as

$$\theta(E,b) = \pi - 2b\int_{r_c}^{\infty} \frac{dr}{r^2\left\{1 - \left[\frac{b^2}{r^2}\right] - \frac{V(r)}{E}\right\}^{\frac{1}{2}}} \tag{21}$$

This integral can be solved analytically in only two cases of interest. One of these is for a hard-sphere collision

$$V(r) = 0,\ r > d;\ V(r) = \infty,\ r \leqslant d \tag{22}$$

where $d$ is the sum of the radii of the two hard-sphere atoms. The result is

$$\cos\frac{\theta}{2} = \frac{b}{d} \tag{23}$$

which we note is independent of $E$. The other case is the repulsive coulomb potential

$$V(r) = \frac{B}{r} \qquad (B > 0) \tag{24}$$

for which

$$\theta(E,b) = 2\sin^{-1}\left[\frac{BE^{-1}}{\{(B/E)^2 + 4b^2\}^{\frac{1}{2}}}\right] \tag{25}$$

For neutral atom scattering we must consider potentials of the type shown in Figure 4a. For large impact parameters the trajectory only experiences the long range part of the potential and in this case trajectories will be bent towards the scattering centre. To preserve continuity between $b$ and $\theta$, the deflection function is defined as a continuous function between $\pi$ and $-\infty$. The general form of $\theta(E,b)$ for collisions in which $E$ is large compared with the depth of the well is as shown in Figure 5.

For atom–atom scattering there is no experimental way of distinguishing between the deflection angles $\theta$ and $-\theta$; only $|\theta|$ can be measured and this is called the scattering angle. Thus in Figure 5 the $b$ values corresponding to the crosses contribute to the same scattering angle.

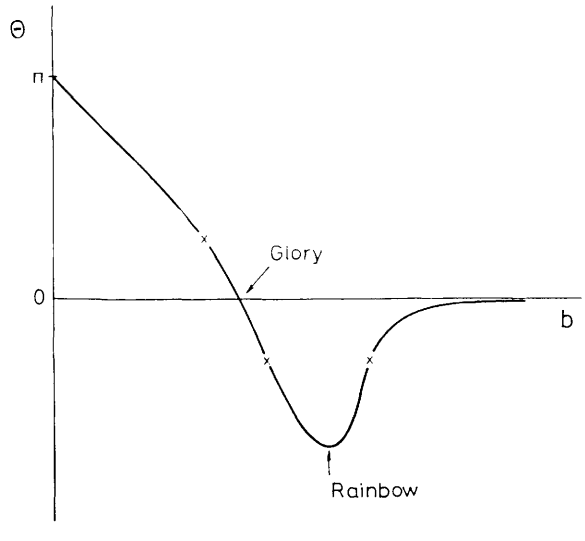


**Figure 5** Typical deflection function for atom–atom potentials when the collision energy is large compared with the well depth. The crosses show the three impact parameters that scatter into $\theta = 50°$.

To calculate a quantity which can be related to experimental measurements we must consider a stream of particles coming in with cylindrical symmetry parallel to the $z$ axis and being scattered into a cone by the scattering centre. Figure 6 illustrates an annulus of the incoming beam with impact parameter lying between $b$ and $b + \mathrm{d}b$, being scattered into a conical section between $\theta$ and $\theta + \mathrm{d}\theta$. Particles crossing the area

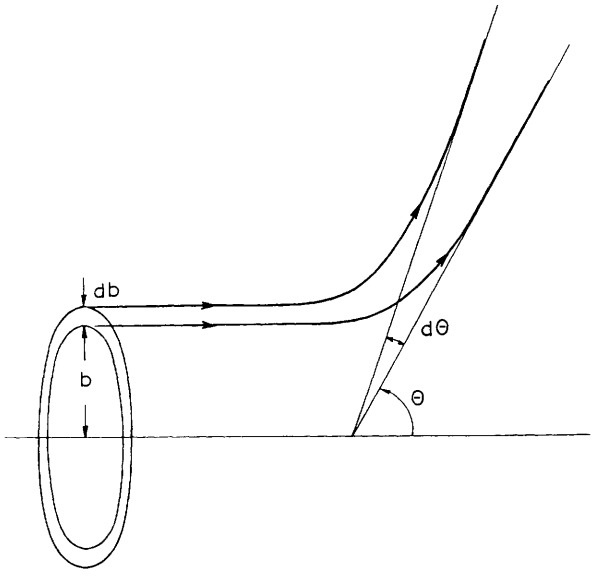


**Figure 6** Parameters for the derivation of the cross-section for central field scattering.

$$dA = 2\pi b db \tag{26}$$

are scattered into the solid angle

$$d\Omega = 2\pi \sin\theta d\theta \tag{27}$$

Results are described by a quantity called the cross-section which is the notional area of the incident beam scattered into a given unit solid angle. As all of the trajectories crossing $dA$ go into the solid angle $d\Omega$, the area that goes into unit solid angle is

$$\sigma(\theta) = \frac{2\pi b db}{2\pi \sin\theta d\theta} \tag{28}$$

This can be rewritten

$$\sigma(\theta) = \left| \frac{b}{\sin\theta \left[\frac{d\theta}{db}\right]} \right| \tag{29}$$

where, by taking the modulus, we allow for the fact that each $b$ value contributes positively to $\theta$ whatever the sign of $\sin\theta$ or $d\theta/db$. If there are several $b$ values contributing to the same scattering angle $\theta$, we add their individual terms such as equation 29. By integrating $\sigma(\theta)$ over $\theta$ we obtain a total cross-section

$$\sigma = \int \sigma(\theta) d\Omega = 2\pi \int_0^{\pi} \sigma(\theta) \sin\theta d\theta \tag{30}$$

If the cross-sections are calculated for the hard-sphere potential from equation 23, we find $\sigma(\theta) = d^2/4$ and $\sigma = \pi d^2$; the latter agrees with our intuitive expectation.

We note that $\sigma(\theta)$ is infinite if either $\sin\theta = 0$ or $(d\theta/db) = 0$. The former is called a glory and the latter a rainbow. Both of these will occur if the potential has both attractive and repulsive branches. However, the classical picture of associating specific trajectories ($b$ values) with each scattering angle is not the whole truth. In quantum mechanics such specificity is forbidden by the uncertainty principle; in a sense each impact parameter gives some contribution to scattering at all angles. Nevertheless, the classical picture is qualitatively correct. Although infinities do not occur in experiments, the presence of strong scattering at certain angles does, and these are associated with the classical glories and rainbows.

## 5 Quantum Scattering by a Central Force

We expect readers to be already familiar with the solution of one central force problem in quantum mechanics, which is the electronic energy levels of the hydrogen atom. The Schrödinger equation for this system is most easily solved by taking spherical polar coordinates as variables and separating the wave function into a product of angular functions and radial functions.

Formally the Schrödinger equation for central force scattering is very similar to that for the hydrogen atom, differing only in the replacement of the coulomb potential between an electron and a proton by the atom–atom potential. For bound-state problems the wave functions must approach zero when $r$ approaches infinity; this condition produces quantization of the energy levels. In the scattering problem the wave functions are not zero at infinity, instead they must represent the atoms coming together initially along straight lines and departing from one another in some angular pattern.

The wave function $\exp(ikz)$ represents a stream of particles moving with momentum $k\hbar$ in the direction of increasing $z$; it is called a plane wave. We can show this by noting that this function is an eigenfunction of the momentum operator $-i\hbar\,(d/dz)$ with eigenvalue $k\hbar$. After the collision, when the atoms are well away from the collision region, we have particles still moving with momentum $k$ but they are moving out in all directions. If the particles were moving isotropically they would be described by a wave function

$$\frac{\exp(ikr)}{r} \tag{31}$$

which is called a spherical wave. The $r$ in the denominator is required to preserve probability within a given solid angle.

To introduce anisotropy into the scattered wave, we use the function

$$\frac{f(\theta)\exp(ikr)}{r} \tag{32}$$

where $f(\theta)$ is called the scattering amplitude. Only one angular variable is needed for central force scattering as the scattering has cylindrical symmetry about the $z$ axis.

We can now establish the boundary conditions on the wave functions through the asymptotic expression

$$\psi \sim e^{ikz} + \frac{f(\theta)e^{ikr}}{r} \tag{33}$$

where $\sim$ indicates the limit as $r \to \infty$. What we do not know is the form of the wave function in the interaction region (where the interatomic potential is non-zero), and to find this we must solve the Schrödinger equation with this boundary condition.

The Schrödinger equation for the system is

$$\left[\frac{-\hbar^2}{2\mu}\nabla^2(\mathbf{r}) + V(r)\right]\psi(\mathbf{r}) = E\psi(\mathbf{r}) \tag{34}$$

and by introducing the variables

$$k^2 = \frac{2\mu E}{\hbar^2},\quad U(r) = \frac{2\mu V(r)}{\hbar^2} \tag{35}$$

this takes the simpler form

$$[\nabla^2 + k^2 - U(r)]\psi(\mathbf{r}) = 0 \tag{36}$$

A general solution to this can be obtained as an expansion in Legendre functions

$$\psi(\mathbf{r}) = \frac{1}{r}\sum_{l=0}^{\infty} A_l \psi_l(r) P_l(\cos\theta) \tag{37}$$

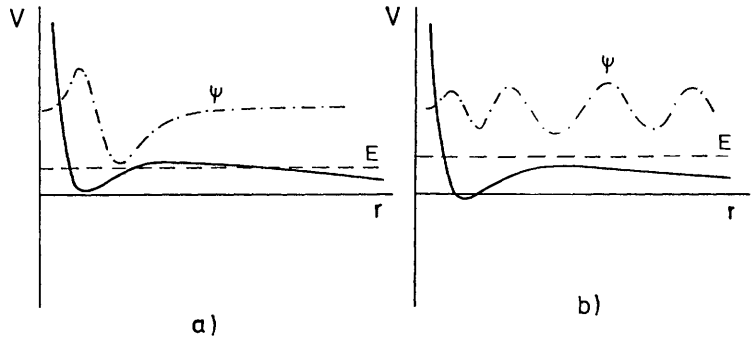


**Figure 7** Radial wave-functions for an Ar–Ar potential.

which is called the partial wave expansion.

On substituting equation 37 into equation 36 we find that the radial wave functions $\psi_l(r)$ are solutions of

$$\left[\frac{d^2}{dr^2} + k^2 - U_l(r)\right]\psi(r) = 0 \tag{38}$$

where

$$U_l(r) = U(r) + \frac{l(l+1)}{r^2} \tag{39}$$

is the effective potential. Notice its close similarity to the effective potential that occurs in classical theory (equation 17), the difference only being the replacement of $L^2$ by $\hbar^2\{l(l+1)\}$, a familiar feature in quantum mechanics.

There are two linearly independent solutions of equation 38 for each value of $k^2$ and $l$. However, only one of these is physically acceptable and that is the one which is zero at $r = 0$; called the regular solution. Figure 7 shows typical functions. When $r$ reaches a value such that $U_l(r)$ can be neglected, the wave functions have the form

$$\psi(r) \sim \sin(kr + \eta_l) \tag{40}$$

However, it can be shown that the centrifugal potential contributes $-l\pi/2$ to the phase $\eta_l$ so the effect of $U(r)$ alone is measured by

$$\delta_l = \eta_l + \frac{l\pi}{2} \tag{41}$$

which is called the phase shift. Broadly speaking, the repulsive regions of $U(r)$ give negative contributions to $\delta_l$ and the attractive regions give positive contributions. Figure 8 shows the dependence of the phase shift on $l$ for the same interatomic potential used for the classical calculation shown in Figure 5.

To derive the relationship between the scattering amplitude $f(\theta)$ and $\delta_l$, we can equate the asymptotic form of equation 37 which is

$$\psi(r) \sim \frac{1}{r}\sum_{l=0}^{\infty} A_l \sin\left(kr - \frac{l\pi}{2} + \delta_l\right) P_l(\cos\theta) \tag{42}$$

with the asymptotic form, which represents the physical situation in the crossed-beam scattering experiment. To do this involves some standard but rather tedious algebra. The result is

$$f(\theta) = \frac{1}{2ik}\sum_{l=0}^{\infty}(2l+1)\,(e^{2i\delta_l} - 1)P_l(\cos\theta) \tag{43}$$

The scattering cross-section can be deduced from the amplitudes of the incident and scattered waves in the asymptotic wave

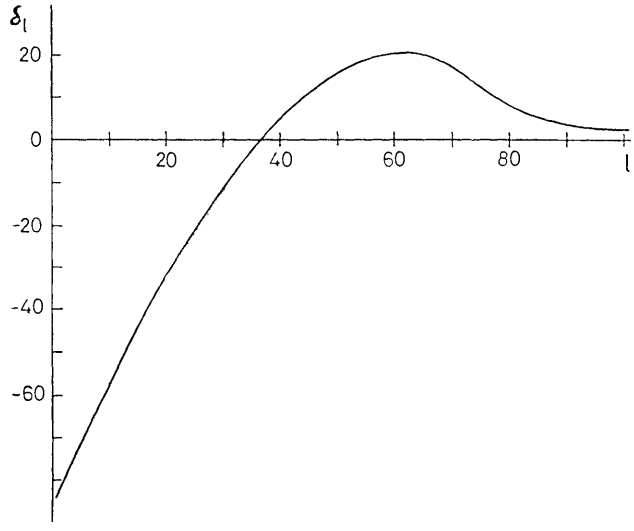


**Figure 8** The variation in $\delta_l$ for an $Ar_2$ potential. The collision energy is twice the well depth.

function. In the incident beam the particles have a probability density

$$|e^{ikz}|^2 = 1 \tag{44}$$

and in the scattered beam the probability density across an area of the sphere which subtends the unit solid angle at the centre is

$$r^2\left|\frac{f(\theta)e^{ikr}}{r}\right|^2 = |f(\theta)|^2 \tag{45}$$

The differential cross-section is the ratio of these two quantities,

$$\sigma(\theta) = |f(\theta)|^2 \tag{46}$$

On replacing $f(\theta)$ by the partial wave expansion (equation 43) we obtain the following expression for the cross-section

$$\sigma(\theta) = \frac{1}{4k^2}\sum_{l=0}^{\infty}\sum_{l'=0}^{\infty}(2l+1)(2l'+1)(e^{-2i\delta_l} - 1) \times (e^{2i\delta_{l'}} - 1)P_l(\cos\theta)P_{l'}(\cos\theta) \tag{47}$$

in which we note that there are interference terms (cross terms) between $l$ and $l'$ partial waves. The expression for the total cross-section is rather simpler because on integrating over $\theta$, we can make use of the orthogonality of the Legendre polynomials so that only the terms with $l = l'$ persist.

$$\sigma = \frac{4\pi}{k^2}\sum_{l=0}^{\infty}(2l+1)\sin^2\delta_l \tag{48}$$

For atomic collisions, at the energies normally encountered in laboratory conditions, one generally needs at least a hundred partial waves to obtain convergence of the cross-sections. An estimate of the maximum value of $l$ which is needed can be obtained from the classical expression equation 20 by comparing the impact parameter with the range of the interatomic potential.

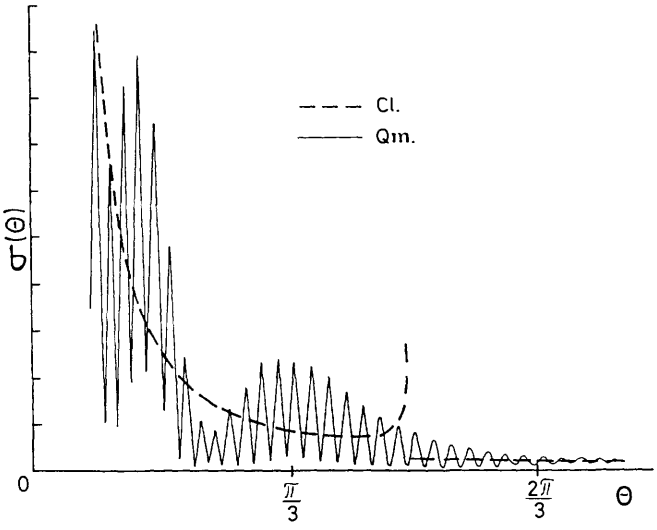


**Figure 9** Quantum and classical cross-sections for atom–atom scattering associated with a deflection function of the type shown in Figure 8. The calculations were made for an $Ar_2$ potential and a collision energy equal to twice the well depth.

Figure 9 compares the quantum and classical cross-sections for Ar–Ar scattering at a collision energy equal to twice the well depth ($\sim 0.04$ eV). Approximately 200 partial waves were needed to obtain convergence. The fine oscillations arise from the cross terms ($l \neq l'$) in equation 47 and the broad oscillation with a peak at $\theta \approx \pi/3$ is associated with the classical rainbow.

When a large number of terms have to be included in the partial wave expansion, a number of approximations can be made to simplify the calculation. Moreover, if one makes use of the semi-classical approximation to the wave function, then one can show that for heavy atom scattering the quantum mechanical cross-section is consistent with the classical expression equation 29.

## 6 Inelastic Collisions; the Classical Picture of Vibrations

Inelastic collisions are important processes for the establishment of equilibrium populations of vibrational and rotational energy levels in gases and liquids. In crossed molecular beam experiments we can study the exchange of translational and rotational energies, so called T–R exchange, or translational and vibrational energies (T–V exchange). Both of these depend mainly on collisions which probe the repulsive part of the inter-molecular potential, and a hard potential model can reproduce many of the important features. The main exception is if there is a strong long-range term in the interaction potential, *e.g.* for ion–dipolar molecule collisions.

Although molecular collisions occur at all orientations, the strongest T–V exchange is expected when atoms collide along the direction of their attached bonds so the collinear atom–diatomic molecule collision is an interesting model. If the atoms are hard, the energy transferred in the collision depends on the phase of the diatomic oscillator at the moment of impact, the largest transfer occurring when the relative velocity of the colliding atoms is largest. Qualitatively, a similar result is obtained if the interaction potential is soft.

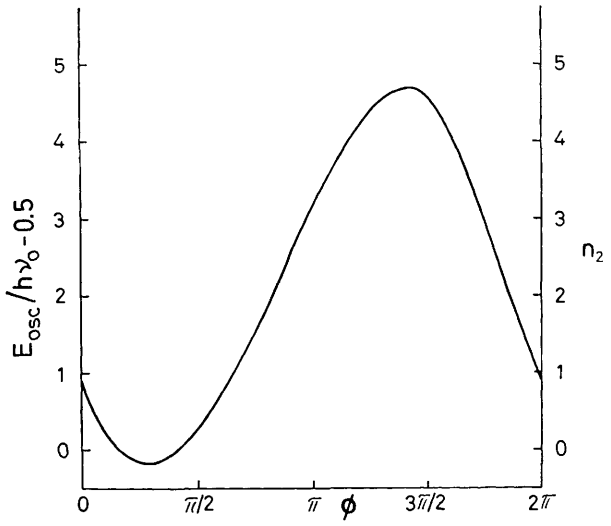


**Figure 10** Relationship between the energy transfer and the oscillator phase for a soft collinear collision with parameters chosen to model He + $H_2$. The initial quantum number is $n_1 = 1$.

Figure 10 shows the results of classical calculations with parameters chosen to model He + $H_2$. The $H_2$ is represented as a harmonic oscillator whose energy can be represented by

$$E_n = (n + \tfrac{1}{2})h\nu \tag{49}$$

although in the classical model, the quantum number $n$ is not restricted to integer values. The interaction potential was taken as an inverse exponential of the distance between the colliding atoms.

The question now arises as to how one should interpret these classical calculations. We can easily deduce an average T–V energy transfer by averaging over the phase $\phi$, but for state-to-state cross-sections we must go further. Two methods have been used; one called quasi-classical, the other semi-classical. In the quasi-classical method one assigns any trajectory that has a final value of $n$ between $k - \frac{1}{2}$ and $k + \frac{1}{2}$ to the quantum state $k$. Thus if we run $N$ trajectories, uniformly or randomly distributed over the initial phase $\phi$, and $N_k$ of these lead to state $k$, then the probability of the transition to $k$ is $N_k/N$.

In the semi-classical picture we pick out those trajectories that end with integer values of $n$. We see from Figure 10 that there are only two values of the phase that lead from $n = 1$ to $n = 2$. If trajectories with phases between $\phi$ and $\phi + \delta\phi$ lead to a final quantum number between $n$ and $n + \delta n$, then the contribution to the probability from this set of trajectories is

$$\frac{1}{2\pi}\left(\frac{\delta\phi}{\delta n}\right) \tag{50}$$

Taking the limit ($\delta \to 0$) and summing over all trajectories leading to the specified final $n$ gives

$$P_n = \Sigma\,[2\pi\left(\frac{\mathrm{d}n}{\mathrm{d}\phi}\right)]^{-1} \tag{51}$$

As we shall see later, this approach taken at the best semi-classical level gives state-to-state transition probabilities which agree quite well with the quantum results.

## 7 The Classical Picture of T–R Exchange

In the collinear collision model we can define transition probabilities but not cross-sections, either total or differential. For this we must have 3D collisions, and these will produce T–R energy transfer. The simplest model is the collision of an atom and a

rigid rotor diatomic molecule, with the interaction potential between these being a 'hard' shape.

Angular momentum is conserved in a collision and for atom–molecule collisions the angular momentum consists of two parts: the orbital angular momentum of the relative motion of the centres of mass (the equivalent of $\boldsymbol{L}$ in elastic scattering) and the rotational angular momentum of the molecule $\boldsymbol{j}$. As both of these are vector quantities, the total angular momentum is $\boldsymbol{J} = \boldsymbol{L} + \boldsymbol{j}$. This vector coupling leads to some standard but rather complicated algebra in the theory of rotational inelasticity. In two dimensions (co-planar collisions), $\boldsymbol{j}$ and $\boldsymbol{L}$ are perpendicular to the plane of motion, and hence the magnitude of the total angular momentum is either $j + L$ or $|j - L|$.

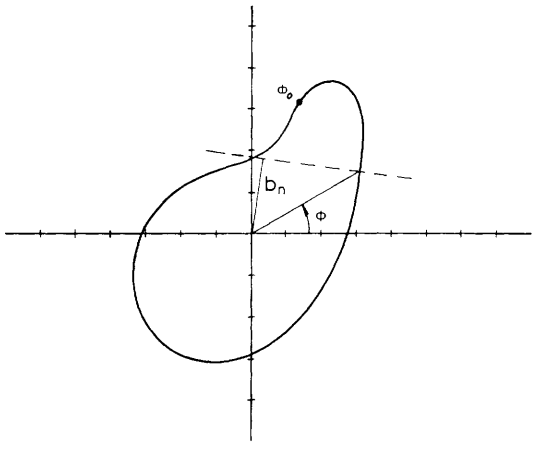


**Figure 11** Effective impact parameter for a two-dimensional hard potential.

Figure 11 shows a 2D hard potential that might apply to the collision of an atom and a small polyatomic molecule. The molecule will have its rotational energy changed by a collision if the impact force (which is perpendicular to the perimeter curve) does not pass through its centre of mass. The torque is proportional to the perpendicular distance from the centre of mass to the line of force; we call this the effective impact parameter $b_n$. Figure 12 shows the function $b_n(\theta)$ for the shape shown in Figure 11. The most important feature is that $b_n(\theta)$ has maxima and minima. Collisions at these points on the perimeter give the largest changes in rotational energy; more important, they dominate the energy change because $b_n$ changes slowly as the point of collision moves away from these points.

If one has a mathematically defined hard shape potential, then from the equations conserving energy and angular momentum,

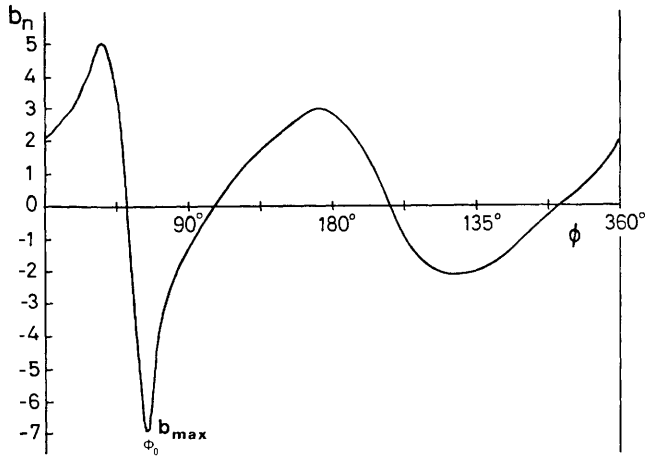


**Figure 12** Effective impact parameter as a function of orientation angle for the potential of Figure 11

the change in rotational angular momentum can be deduced for different scattering angles as a function of $b_n$. Cross-sections can then be deduced for each pair of initial and final rotational states of the molecule (characterized by $j_i$ and $j_f$). The relevant formula is a generalization of that given for elastic scattering (equation 29) ($\alpha$ is the initial angle of the molecule relative to the line of collision).

$$\sigma_{if}(\theta) = \left(\frac{v_f}{v_i}\right) b_n \left[\frac{\partial\theta}{\partial b_n}\frac{\partial j_f}{\partial\alpha} - \frac{\partial\theta}{\partial\alpha}\frac{\partial j_f}{\partial b_n}\right]^{-1} \tag{52}$$

As for elastic scattering this expression has the possibility of singularities when the two terms appearing in the square brackets are zero or cancel. These so-called rotational rainbows appear as dominant features of the differential cross-sections for each pair of initial and final states, although, as with elastic scattering, quantum mechanics will smooth out the classical infinities.

## 8 Quantum Mechanics of Inelastic Scattering

For molecular scattering the wave function depends on the vector $\boldsymbol{r}$ of relative motion of the two centres of mass and on a set of internal variables $\boldsymbol{s}$ which are associated with the vibrational and rotational states of the molecules. As $r$ approaches infinity the interaction potential $V(r,\boldsymbol{s})$ approaches zero and the wave functions can be written as products of continuum functions for the relative motion and the wave functions for the discrete internal states.

It is not possible to obtain the asymptotic form of the scattering wave function by direct numerical integration of the many-dimensional Schrödinger equation with this boundary condition. The procedure normally followed is the one used to find the bound states of many-dimensional systems with non-separable potentials, namely to make an expansion of the wave function in a set of known functions, which is called the basis set (*e.g.* the well known LCAO expansion in molecular orbital theory). For scattering wave functions the basis covers only the internal variables $\boldsymbol{s}$.

Two types of basis are commonly used, one depending only on $\boldsymbol{s}$ and the other that depends on both $r$ and $\boldsymbol{s}$. The former leads to what is called the diabatic representation of the wave function and the latter to an adiabatic representation. Adiabatic bases are more complicated functions and may be difficult to obtain, but to compensate for this one should need fewer of them to provide a specified computational accuracy.

Both the diabatic and adiabatic sets must represent the eigenfunctions for the internal motion of the molecules in the asymptotic region. Thus if the diabatic set are the functions $\chi_j(\boldsymbol{s})$ the adiabatic set $\Lambda_j(r,\boldsymbol{s})$ will satisfy the condition

$$\lim_{r\to\infty} \Lambda j(r,\boldsymbol{s}) = \chi_j(\boldsymbol{s}) \tag{53}$$

To derive the multi-channel equations we write the total Hamiltonian as

$$H = -\frac{\hbar^2}{2\mu}\nabla^2(\boldsymbol{r}) + V(r,\boldsymbol{s}) + H^0(\boldsymbol{s}) \tag{54}$$

where the interaction potential $V$ depends only on the scalar distance between the interacting species; it is of course dependent on the orientations of the molecules relative to $\boldsymbol{r}$, but these angles are in the set of internal coordinates $\boldsymbol{s}$.

In the diabatic basis we expand the total wave function as

$$\psi(\boldsymbol{r},\boldsymbol{s}) = \sum_j \psi_j(r)\chi_j(\boldsymbol{s}) \tag{55}$$

where $\chi_j(\boldsymbol{s})$, the eigenstates of $H^0$, are an orthonormal set satisfying

$$H^0(\boldsymbol{s})\chi_j(\boldsymbol{s}) = E^0{}_j\chi_j(\boldsymbol{s}) \tag{56}$$

The Schrödinger equation then takes the form

$$\sum_i [-\frac{\hbar^2}{2\mu}\nabla^2(\boldsymbol{r}) + V(r,s) + H^0(s) - E]\psi_k(\boldsymbol{r})\chi_i(s) = 0 \qquad (57)$$

This can be converted to a set of coupled equations in $\boldsymbol{r}$ by multiplying in turn by each of the basis functions and integrating over $s$. Making use of the orthogonality of the basis, a typical equation is

$$[-\frac{\hbar^2}{2\mu}\nabla^2(\boldsymbol{r}) + E_i^0 - E + V_{ii}(r)]\psi_i(\boldsymbol{r}) + \sum_{j\neq i} V_{ij}(r)\psi_j(\boldsymbol{r}) = 0 \qquad (58)$$

where

$$V_{ij}(r) = \langle \chi_i(s) \mid V(r,s) \mid \chi_j(s)\rangle \qquad (59)$$

Equations 58 and 59 are called the multi-channel equations. They can be thought of as a set of elastic equations, one for each basis function, which are coupled together by off-diagonal elements of the interaction potential $V_{ij}(\boldsymbol{r})$; $V_{ii}$ and $E_i^0$ are called the channel potentials and channel energies respectively.

Similar equations are obtained from an adiabatic basis. The basis functions are in this case defined by

$$[H^0(s) + V(\mathrm{r},s)]\Lambda_i(r,s) = E_i(r)\Lambda_i(r,s) \qquad (60)$$

and if one substitutes

$$\psi(\boldsymbol{r},s) = \sum_i \psi_i(\boldsymbol{r})\Lambda_i(r,s) \qquad (61)$$

into the Schrödinger equation and forms matrix elements with the basis functions, one gets a set of coupled equations in which the coupling arises from the kinetic energy operator $\nabla^2(\boldsymbol{r})$.

Both the diabatic and adiabatic expansions provide, in principle, an exact description of the wave function; in quantum mechanical terms we say the bases are complete. However, in practice we must take a finite rather than an infinite number of terms in the expansions. The finite set of multi-channel equations is called the close-coupling equations.

To progress further with the coupled channel equations for full three-dimensional scattering we have to make a partial wave expansion of $\psi(\boldsymbol{r})$. This leads to rather complicated equations which reflect the fact that the orbital angular momentum of one molecule around the other is coupled with the rotational angular momenta of the molecules, only the total of these being conserved. However, no such complications arise for the collinear collision model of vibrational inelasticity so we will briefly look at this example for the collinear collision A + BC discussed in Section 7.

With the diabatic basis we must evaluate matrix elements such as

$$V_{ij}(r) = \langle \chi_i(R_{\mathrm{BC}}) \mid \exp(-kR_{\mathrm{AB}}) \mid \chi_j(R_{\mathrm{BC}})\rangle \qquad (63)$$

where the $\chi_i(R_{\mathrm{BC}})$ are harmonic oscillator eigenfunctions. In this expression $r$ is the distance between A and the centre of mass of BC. Taking the case where B and C have equal masses, for simplicity, we have

$$R_{\mathrm{AB}} = r - \tfrac{1}{2}R_{\mathrm{BC}} \qquad (64)$$

so that when the integration over $R_{\mathrm{BC}}$ is carried out the result is a function of $r$. This is where the coupling arises from; if the interaction potential were an exponential in $r$ alone, there would be no T–V exchange.

We will not give details of how the multi-channel equations are solved beyond the fact that one integrates numerically from $r = 0$ out to a sufficiently large value that the scattering wave functions are strictly periodic, and this is done for each of the internal states in turn. As $r$ goes to $\infty$ the wave function picks up contributions from other internal states. This complete set of wave functions (one for each internal state) is then taken in linear combinations so as to match the asymptotic condition required of the scattering wave function. If we want a wave function that represents the system in an initial internal state $i$, emerging in final states $j$, then we write the $j$th component of this wave function (*i.e.* the function $\psi_j(r)$ in equation 55 as

$$\psi_j(r) \sim \delta_{ij}e^{-ik_ir} - S_{ji}\left(\frac{k_i}{k_j}\right)^{\frac{1}{2}}e^{ik_jr} \qquad (65)$$

We have an incoming wave which is non-zero only for the $i$th component, and outgoing waves $\exp(ik_jr)$ for all energetically accessible channels. Channels are characterized by their wave vectors $k$ which, from equation 35, are defined by

$$k_j = \left(\frac{2\mu(E - E_j^0)}{\hbar^2}\right)^{\frac{1}{2}} \qquad (66)$$

If the total energy $E$ is greater than the channel energy $E_j^0$ the transition $i \rightarrow j$ is allowed in the collision; $k_j$ is real and we say the channel is open. If $E$ is less than $E_j^0$, $i \rightarrow j$ is energetically forbidden, $k_j$ is imaginary, and the channel is closed. Although closed channel functions may be included in the basis (in equation 56) to improve accuracy in the interaction region, they must have zero amplitudes in the asymptotic wave functions.

$S_{ji}$ are elements of a matrix called the scattering or $\boldsymbol{S}$ matrix. The factor $(k_i/k_j)^{\frac{1}{2}}$ is also included in the amplitude so that the square modulus of $\boldsymbol{S}$ gives directly fluxes of particles not just probability densities; note that the ratio of velocities appeared in equation 53 for the classical cross-section for the same reason.

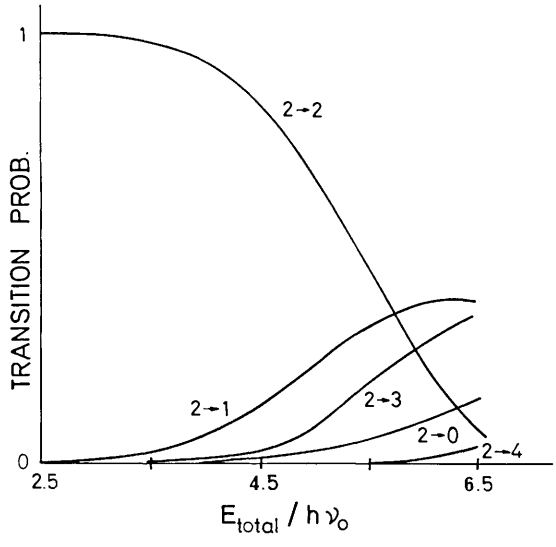


**Figure 13** Quantum mechanical transition probabilities for the collinear collision of an atom and a harmonic oscillator with parameters modelled on He + $H_2$($\alpha = 0.314$, $m = 2/3$).

Figure 13 shows the transition probabilities calculated for He + $H_2$, with the $H_2$ being initially in the quantum state $n = 2$, as a function of the collision energy. Channels 0 and 1 are open at all energies, but note that the probability for $2 \rightarrow 1$ is considerably greater than $2 \rightarrow 0$. Channel 3 becomes open at $E = 3.5h\nu_0$ ($h\nu_0$ being the harmonic oscillator interval) and $2 \rightarrow 4$ at $4.5h\nu_0$. The transition probabilities increase slowly for energies in excess of the threshold, and the elastic component $2 \rightarrow 2$ decreases accordingly to conserve total probability.

Table 1 compares transition probabilities for several initial and final states as calculated by quantum, classical, and semi-classical methods. Of the two semi-classical methods the simpler is the one described earlier in this review and the uniform is a better approximation to the quantum mechanical results, as is evident from the results. Note particularly some cases where the

**Table 1** Transition probabilities for $He-H_2$ collisions at an energy of $10h\nu_0$ ($\sim 4.5$ eV)

| Transition | | Quantum | Classical | Semi-classical | |
|---|---|---|---|---|---|
| $n_1$ | $n_2$ | | | Simple | Uniform |
| 0 | 0 | 0.060 | 0 | 0 | 0.058 |
| 0 | 1 | 0.218 | 0.356 | 0.472 | 0.211 |
| 0 | 2 | 0.366 | 0.212 | 0.416 | 0.381 |
| 0 | 3 | 0.267 | 0.232 | 0.359 | 0.266 |
| 0 | 4 | 0.089 | 0 | 0 | 0.075 |
| 1 | 1 | 0.286 | 0.158 | 0.290 | 0.287 |
| 1 | 2 | 0.009 | 0.130 | 0.009 | 0.011 |
| 1 | 3 | 0.170 | 0.128 | 0.168 | 0.174 |
| 1 | 4 | 0.240 | 0.159 | 0.285 | 0.240 |
| 1 | 5 | 0.077 | 0 | 0 | 0.062 |
| 2 | 2 | 0.366 | 0.212 | 0.416 | 0.381 |
| 2 | 3 | 0.018 | 0.105 | 0.020 | 0.017 |
| 2 | 4 | 0.169 | 0.114 | 0.165 | 0.170 |
| 2 | 5 | 0.194 | 0.169 | 0.262 | 0.194 |
| 2 | 6 | 0.037 | 0 | 0 | 0.045 |

The table is taken from reference 2 where a fuller description is given of the calculations and references to the original work.

classical and simple semi-classical transition probabilities are zero; Figure 14 shows, for example, that $1 \rightarrow 5$ is forbidden. However, these channels are open by the criterion of equation 65 and we can attribute their transition probabilities to the tunnel effect (*i.e.* trajectories that are not classical because they must pass into regions where the potential energy is greater than the total energy. The uniform approximation of semi-classical theory allows for the effect of these non-classical trajectories.

For the collinear collision problem one may typically need about ten basis functions to obtain convergence in the $\boldsymbol{S}$ matrix elements, but for rotational inelasticity a hundred or more would be typical. There are two reasons for this. First, at the collision energies normally met in experiment many rotational channels are likely to be open. Secondly, in a collision, particularly one with a hard intermolecular potential, the free rotor basis functions are individually poor representations of the motion at the point of impact; typically the motion here is libration rather than rotation.

There has been a great deal of interest in finding approximate solutions to the multi-channel equations which are computationally less demanding. The first method to be explored was an iterative solution suggested by Born. Unfortunately, in practice convergence is usually very slow for molecular collisions.

The most commonly used approximations to the multi-channel equations come under the description 'sudden', the term implying that the inelastic processes occur in a time that is short compared with the periods of internal motion. Mathematically the situation is this: if one could find a linear combination of the basis functions such that the potential energy matrix $V_{ij}(r)$ was diagonal, we would have removed this source of coupling, but it would be at the expense of introducing off-diagonal coupling terms in $E_i^0 - E$. However, if the total energy is large compared with the internal energies of the states that are populated, then we can replace all the $E_i^0 - E$ by some average ($\Delta E$) and in that case after diagonalizing $V$, $\Delta E$ will still only appear on the diagonal. Likewise, in 3D scattering one has a centrifugal term on the diagonal $l(l+1)r^2$ and if this is replaced by an average $\overline{l(l+1)}/r^2$, then after diagonalizing $V$ one still has a diagonal centrifugal matrix. One can therefore derive approximations which are so-classed energy-sudden, or centrifugal-sudden, or with both approximations, infinite-order-sudden (IOS). The latter is very commonly employed and, in some cases, has proved to be quite accurate.

Finally, we should mention the fact that the quantum mechanics of collisions over hard potentials can be carried out without great computational difficulty. For atom–atom scattering the solution was found in the early 1930s, but for atom–molecule, rotational inelasticity, such calculations are much more recent.[3] Although one does not avoid the use of multi-channel equations in this approximation, the calculations are easier because the coupling only occurs at the potential wall, and not over a wide range of $r$; it is in this sense properly described as sudden.

## 9 Reactive Scattering

Reactive scattering is a category of inelastic scattering in which the internal states depend on the manner in which the atoms are grouped together in the initial and final states. For example, in the simple atom–diatomic molecule exchange reaction represented symbolically as

$$A + BC \rightarrow AB + C \qquad (67)$$

the internal states will be both BC states and AB states, and if there is also the possibility of forming AC molecules or of having sufficient energy in the reaction to give A + B + C, then these must be added to the list of internal states.

The quantum mechanical treatment of inelastic scattering relies for its success on finding good basis functions for the internal states. A prerequisite for this is that the coordinates can be separated into an internal set $s$ and scattering coordinates $r$. It is obviously much more difficult to make such a separation when the internal states encompass reaction than when they do not. Because of this the quantum mechanical treatment of reactive scattering is much more difficult than that of inelastic non-reactive scattering.

There are two approaches to the coordinate problem. One of these is to use different coordinates for the reactants and product regions of $s$. In this case, the basis functions which describe the internal states must change with the coordinates and it will be necessary to maintain continuity of the wave functions at boundaries in the interaction region. The second method is to use coordinates which cover the whole space but which are not linear transformations of either the reactant or product coordinates. In this case the best coordinates may depend on the specific problem to be solved. The best known of these is the Marcus 'natural coordinate system' for collinear collisions which is illustrated in Figure 14. The reaction coordinate, $\rho_r$, is a curve which follows the bottom of the reactant valley, passes over the saddle point and exits along the bottom of the product valley. The internal coordinate $\rho_x$ is a vector perpendicular to $\rho_r$ at all points. In this figure the reactant and product valleys have been drawn in so-called skew coordinates with

$$\cos\beta = \left[\frac{m_A m_C}{(m_B + m_C)(m_B + m_A)}\right] \qquad (68)$$

so that the classical expression for the kinetic energy contains no cross terms $\dot{X}\dot{Y}$.

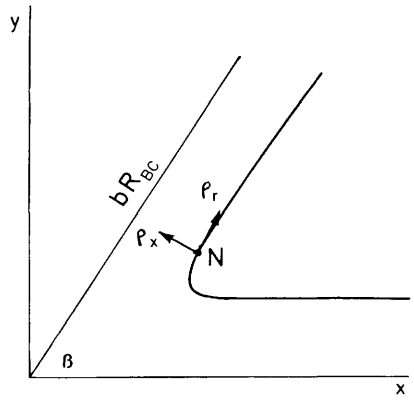


**Figure 14** The Marcus natural reaction coordinates.

The Marcus system has the advantage that it can be tailored to the potential so that full use can be made of any separable approximations to the potential. However, there are disadvantages; particularly non-uniqueness in some regions. Other curvilinear systems have been proposed based on transformations of rectilinear variables that are independent of the potential function. One of these is that of Delves which was developed for use in nuclear physics. Starting from a system in which the kinetic energy is separable, a transformation is made to polar coordinates such that

$$X = r\cos\alpha, \qquad Y = r\sin\alpha \tag{69}$$

with $\alpha$ being defined in the range 0 to $\beta$ (the skew angle).

Delves' coordinates in polar form are particularly suitable for describing the heavy–light–heavy triatomics for which the skew angle $\beta$ is small. They can also be generalized for higher dimensions and become what are known as hyperspherical coordinates. If there are $n$ dimensions, a coordinate set can always be found in which there is only one distance variable, $r$, and the other $n - 1$ variables are all angles.

The advantage of hyperspherical coordinates is that all the reaction and product channels are at $r = \infty$ and are distinguished by different values of the angular variables. Thus $r$ can be taken as a scattering coordinate for all reactive or non-reactive processes. The disadvantage of hyperspherical coordinates is that the contours of the potential do not follow the lines of constant $r$ or constant angle, so there are very strong coupling terms in the potential energy for such a system.

The choice of variables is a problem for quantum mechanics because the wave functions have to satisfy boundary conditions which are different for different variables. In classical mechanics the matter is much less important because the equations determining the classical trajectories can be integrated numerically in any coordinate system, although there are advantages in having variables that change slowly with time. The classical treatment of reactive scattering is much the simpler and we therefore turn now to this technique.

In the classical trajectory method one examines a batch of trajectories, with initial conditions chosen randomly and makes a statistical analysis of the outcome; this is called the Monte Carlo method. The number of trajectories that have to be examined depend on the questions being asked. For example, if one takes a batch of $N$ trajectories, all conforming with equal weight to certain initial conditions, and if $N_r$ lead to reaction and $N - N_r$ to no reaction, then the probability of reaction is

$$P = \frac{N_r}{N} \tag{70}$$

and the standard error of this result is

$$\epsilon = \left(\frac{N - N_r}{NN_r}\right)^{\frac{1}{2}} \tag{71}$$

which is roughly proportional to $N^{-\frac{1}{2}}$ if $N_r/N$ is a reasonably large fraction. To double the accuracy of a result one needs to increase the number of trajectories by a factor of four. However, if $N_r/N$ is small, the error is proportional to $N_r^{-\frac{1}{2}}$; hence one needs more trajectories to obtain a given level of accuracy for improbable events, *e.g.* if one is interested in knowing what is the probability of a product being in a particular vibrational and rotational energy state.

If one considers the initial conditions for an A + BC trajectory, then in the centre-of-mass coordinate system we have twelve conditions to be specified. Some of these will be determined by the initial state of the reactants, some will be arbitrary (arising from an arbitrary choice of axes) and others will be chosen randomly so as to simulate the whole range of collisions that can occur. For example, in an ideal state-selected crossed-beam experiment BC would be in a well-defined vibrational–rotational state so the quantum numbers $v$ and $j$ will determine two of our twelve initial conditions. A third is given by the relative velocity of A to the centre of mass of BC.

The initial value of the $y$ relative position coordinate is the impact parameter $b$. In a real collision any value of $b$ is possible but the probability of reaction will fall to zero as $b$ goes to infinity. In general there is a sharp decrease in the probability of reaction beyond a certain value of $b$ and by running a small number of trajectories one can establish a minimum value of $b$ beyond which no reaction occurs; this is typically a few angstroms. This minimum value gives the upper limit of $b$, called $b_{max}$, which has to be sampled in a batch of trajectories in order to simulate all feasible reactive collisions. The usual procedure for selecting the $b$ value for a trajectory is to generate a random number, $\zeta$, between zero and one and to take

$$b = \zeta b_{max} \tag{72}$$

As the area of the cross-section between $b$ and $b + db$ is $2\pi b db$ one must weight the result of each trajectory by its $b$ value.

Finally, one has initial conditions arising from the orientation of BC and the phase of the BC vibration at the start of the trajectory and these also must be chosen randomly with appropriate weighting. When the trajectory is completed, the coordinates and momenta must be transformed to the appropriate products and analysed to give the distribution of energy between the relative translational motion and the vibrational and rotational motion of the diatomic species. The scattering angle in the centre-of-mass coordinate system will be given by the angle between the incoming vector $v_r$ and the equivalent outgoing vector for the relative translational motion. From the vibrational and rotational energies we can determine semi-classical quantum numbers $v'$ and $j'$, and these can be discretized by rounding them to the nearest integer number, as discussed for inelastic scattering.

The probability of reaction to particular products for specific values of $v_r$, $v$, $j$, and $b$ is called the opacity function, $P_R$. The reaction cross-section is then

$$\sigma_R(v_r,v,J) = 2\pi\int_0^{b_{max}} P_R(v_r,v,J,b)b\,db \tag{73}$$

Equation 73 is the cross-section for reactions that proceed over the particular potential energy surface on which the trajectories have been calculated. A further complication is that for most reactive systems there is more than one surface that emanates from the state of the reactants, and the total cross-section is the appropriate average for motion on all of these. For example, in the reaction

$$Cl(^2P) + O_2(^3\Sigma_g^-) \rightarrow ClO(^2\Pi) + O(^3P) \tag{74}$$

the total electronic degeneracy of the reactants is six for Cl and three for $O_2$, so that there are eighteen different electronic states that are asymptotic to these reactants. The ground-state surface of $ClO_2$ is a doublet but has no orbital degeneracy, so that only one in nine collisions of the reactants will pass over the ground-state surface. If the reaction only proceeds over the ground-state surface, which would be the case if all the excited-state surfaces had high barriers to the formation of products, then to compare the calculated cross-section with experimental quantities one would have to multiply equation 73 by a degeneracy factor of 1/9.

In any experiment, even in a molecular beam reaction, there will be some averaging over $v_r$, $v$, and $j$. It follows that cross-sections such as equation 73 must be weighed by state populations in order to compare calculated and experimental results. By applying Maxwell–Boltzmann statistics for the state populations and velocity distributions in an equilibrium gas, one can determine thermally averaged rate constants from cross-sections.

The quantum theory of reactive scattering is currently an area of intense research activity so we give only an outline of the most popular approach.

We have already stressed the difficulty of defining coordinates and basis functions for reactive scattering. Another problem is that there are frequently a large number of open channels. This is particularly true for reactions which must surmount a potential energy barrier because this can entail a large energy release in the reaction channels with the product molecules produced in a wide range of rotational and vibrational states. The number of multichannel equations that have to be integrated is usually much higher than in a typical inelastic scattering problem.

It is not surprising that the most intensely studied problem is the $H + H_2$ isotope exchange reaction. This system has the advantage of a small activation barrier and a large rotational spacing, so that close to the reaction threshold only a few rotational channels are open. We will pass over the early studies of the collinear model for this reaction, although they were in their time important. Wolken and Karplus[4] were the first to solve the multi-channel equations for the reaction in 3D using a small rotational basis ($j = 0$ to 6) for reactants and products, only the ground vibrational states, and values of the total angular momentum up to 12. Different coordinates were used for each reaction channel and a transformation from one to the other made in the interaction region. The main conclusion from this work was that the threshold for reaction was considerably lower than that found from classical trajectory calculations due to tunnelling through the barrier.

The simple view of tunnelling is that it is the passage of particles into regions where the potential energy is greater than the total energy; in consequence the momentum is imaginary in these regions. However, of equal importance is the zero-point vibrational energy of the system, because this changes as the system evolves on the potential energy surface. Calculations on 1D and 2D models of the $H + H_2$ reaction show that the threshold energy increases by about 0.06 eV with each additional dimension, and this is approximately equal to the zero-point energy for the bending mode of the $H_3$ transition-state structure.

Many current quantum calculations on reactive systems use hyperspherical coordinates. These were first employed for $H + H_2$ by Kuppermann and co-workers[5] on the collinear reaction. Schatz[6] later used the method for 3D calculations on this system and on $Cl + HCl$ collisions, systems with very different $\beta$ values, and showed it worked well. However, the field is developing so rapidly that one cannot yet do it justice in a review. Zhang and Miller[7] have given a valuable list of references to work carried out until 1989.

## 10 References


1 M. Rigby, E. B. Smith, W. A. Wakeham, and G. C. Maitland, 'The Forces between Molecules', Clarendon Press, Oxford, 1968.
2 J. N. Murrell and S. D. Bosanac, 'Introduction to the Theory of Atomic and Molecular Collisions', John Wiley, Chichester, 1989.
3 S. D. Bosanac and J. N. Murrell, *J. Chem. Phys.*, 1991, **94**, 1167.
4 G. Wolken and M. Karplus, *J. Chem. Phys.*, 1974, **60**, 351.
5 A. Kupperman, J. A. Kaye, and J. D. Dwyer, *Chem. Phys. Lett.*, 1980, **74**, 257.
6 G. C. Schatz, *Chem. Phys. Lett.*, 1988, **92**, 150.
7 J. Z. H. Zhang and W. H. Miller, *J. Chem. Phys.*, 1989, **91**, 1528.


## 11 Bibliography


1 M. S. Child, 'Molecular Collision Theory', Academic Press, London and New York, 1974.
2 R. D. Levine and R. B. Bernstein, 'Molecular Reaction Dynamics and Chemical Reactivity', OUP, Oxford, 1987.
3 R. B. Bernstein, 'Introduction to Atom–Molecule Collisions: The Interdependency of Theory and Experiment', in 'Atom–Molecule Collision Theory: A guide for the Experimentalist', ed. R. B. Bernstein, Plenum Press, New York, 1979.
4 U. Buck, 'Elastic Scattering', *Adv. Chem. Phys.*, 1975, **30**, 313.
5 E. E. Nikitin, 'Theory of Elementary Atomic and Molecular Processes in Gases', Clarendon Press, Oxford, 1974.
6 J. P. Toennies, 'Molecular Beam Scattering Experiments on Elastic, Inelastic, and Reactive Collisions' in 'Physical Chemistry', Vol. 6, ed. H. Eyring, W. Jost and D. Henderson, Academic Press, New York, 1974—5.
7 M. V. Berry and K. E. Mount, 'Semi-classical Approximations in Wave Mechanics', *Rep. Prog. Phys.*, 1972, **35**, 315.
8 R. E. Johnson, 'Introduction to Atomic and Molecular Collisions', Plenum Press, New York, 1982.
9 'Molecular Beam Scattering', ed. K. P. Lawley, *Adv. Chem. Phys.*, 1975, **30**, 1.
10 H. S. W. Massey, 'Atomic and Molecular Collisions, Taylor and Francis, London, 1979.
11 N. F. Mott and H. S. W. Massey, 'The Theory of Atomic Collisions', Clarendon Press, Oxford, 1965.
12 H. Pauly, 'Elastic Scattering Cross-sections', in 'Atom–Molecule Collision Theory: A Guide for the Experimentalist', ed. R. B. Bernstein, Plenum Press, New York, 1979.
13 A. E. De Pristo and H. Rabitz, 'Vibrational and Rotational Collision Processes', *Adv. Chem. Phys.*, 1985, **42**, 271.
14 A. S. Dickinson, 'Non-reactive Heavy Particle Collision Calculations', *Comp. Phys. Commun.*, 1979, **17**, 51.
15 G. A. Fisk and F. F. Crim, 'Single Collision Studies of Vibrational Energy Transfer Mechanics', *Acc. Chem. Res.*, 1977, **10**, 73.
16 W. R. Gentry, 'Vibrational Excitation: Classical and Semi-classical Methods', in 'Atom–Molecule Collision Theory: A Guide for the Experimentalist', ed. R. B. Bernstein, Plenum Press, New York, 1979.
17 D. Rapp and T. Kassal, 'The Theory of Vibrational Energy Transfer between Simple Molecules in Non-reactive Collisions', *Chem. Rev.*, 1969, **69**, 61.
18 D. Secrest, 'Theory of Rotational and Vibrational Energy Transfer in Molecules', *Ann. Rev. Phys. Chem.*, 1973, **24**, 379.
19 H. K. Shin, 'Vibrational Energy Transfer', in 'Dynamics of Molecular Collisions', ed. W. H. Miller, Plenum Press, New York, 1976.
20 'Molecular Collision Dynamics', ed. J. M. Bowman, Springer-Verlag, Berlin, 1983.
21 M. Faubel and J. P. Toennies, 'Scattering Studies of Rotational and Vibrational Excitation in Molecules', *Adv. At. Mol. Phys.*, 1977, **13**, 229.
22 D. J. Kouri, 'Rotational Excitation', in 'Atom–molecule collision theory: A Guide to the Experimentalist', ed. R. B. Bernstein, Plenum Press, New York, 1979.
23 H. J. Loesch, 'Scattering of Non-spherical Molecules', *Adv. Chem. Phys.*, 1989, **42**, 421.
24 J. P. Toennies, 'The Calculation and Measurement of Cross-sections for Rotational and Vibrational Excitation', *Ann. Rev. Phys. Chem.*, 1976, **27**, 225.
25 M. Baer, 'The Theory of Chemical Reaction Dynamics', CRC Press, Boca Raton, Fl., 1985.
26 'The Theory of Chemical Reaction Dynamics', ed. D. C. Clary, Reidel, Boston, 1986.
27 W. H. Miller, 'Reaction Path Models for Polyatomic Reaction Dynamics – from Transition State Theory to Path Integrals', in 'The Theory of Chemical Reaction Dynamics', ed. D.C. Clary, Reidel, Boston, 1986.
28 J. T. Muckerman, 'Applications of Classical Trajectory Techniques to Reactive Scattering', in 'Theoretical Chemistry', ed. D. Henderson, Academic Press, New York, 1981.
29 R. N. Porter, 'Molecular Trajectory Calculations', *Ann. Rev. Phys. Chem.*, 1974, **25**, 317.
30 L. M. Raff and D. L. Thompson, 'Classical Trajectory Approach to Reactive Scattering', in 'The Theory of Chemical Reaction Dynamics', ed M. Baer, CRC Press, Boca Raton, Fl., 1985.
31 G.C. Schatz, 'Overview of Reactive Scattering', in 'Potential Energy Surfaces and Dynamics Calculations', ed. D. G. Truhler, Plenum Press, New York, 1981.